

Navier-Stokes Calculations of Inboard Stall Delay Due to Rotation

J. C. Narramore*

Bell Helicopter Textron, Inc., Fort Worth, Texas 76101
and

R. Vermeland†

CRAY Research, Inc., Mendota Heights, Minnesota 55120

Momentum blade element methods, which have historically been used to predict rotor blade thrust, underpredict the power that is required for highly twisted rotors at high thrust levels. During a test of the V-22 tilt rotor blade conducted at the NASA Ames Research Center Outdoor Aerodynamic Research Facility (OARF), measurements of the thrust as a function of collective angle showed that the thrust levels achieved were higher than anticipated and drag levels at the high thrust levels were much lower than predicted. Because the maximum thrusting capability of the rotor in hover usually determines the maximum payload of the vehicle, it is important to be able to accurately predict high thrust performance characteristics. A three-dimensional Navier-Stokes method was used to investigate the flow phenomenon that causes the increase in lift coefficients and reduction in drag coefficients obtained near the stall of a rotating blade. Comparison of the computational results with the experimental data indicates that this method can be used to predict thrust levels. The Navier-Stokes results indicate that flow separation near the hub is curtailed for a rotating blade compared with the momentum blade element predictions.

Nomenclature

M	= reference Mach number
P	= pressure
Re	= reference Reynolds number
r/R	= nondimensional radial location
u	= x component of velocity
v	= y component of velocity
w	= z component of velocity
X_r	= x velocity of a grid point
Y_r	= y velocity of a grid point
Z_r	= z velocity of a grid point
ζ	= transformed spanwise coordinate
η	= transformed normal coordinate
ξ	= transformed wraparound coordinate
τ	= time relative to blade-fixed system
ω	= angular velocity of the blade

Introduction

TO develop rotorcraft vehicles with improved performance, accurate prediction and explanation of high thrust performance characteristics are required. Current state-of-the-art performance methods are based on momentum element theories that underpredict rotor lifting capabilities at conditions when the rotor is at or near stall.¹ In a recent large-scale rotor test, stall was delayed, and measured rotor performance was increased compared with computed blade element momentum lifting-surface theory results at high thrust levels.² Figure 1, a comparison between the rotor figure of merit measured on the NASA Ames OARF test stand and a

blade element momentum lifting-surface method (AR7906), shows that at high thrust levels, the momentum element method greatly overpredicts the drag that was measured during the test. The momentum element method predicts an early stall on the inboard region of the blade that causes a significant increase in drag and reduction in lift.

The aerodynamic flowfield about rotorcraft vehicles in hover and low-speed flight is very complicated. To predict performance characteristics of an isolated blade in hover, three-dimensional, compressible, separated, nonlinear, viscous flow phenomena must all be modeled. Current blade element performance codes use only two-dimensional airfoil data to model some of these highly nonlinear characteristics. In recent years, interest has been generated in highly loaded rotor blades due to the advent of the V-22 tilt rotor vehicle and the desire to produce high-maneuverability helicopters. Thus, there is a desire to be able to predict more accurately the performance

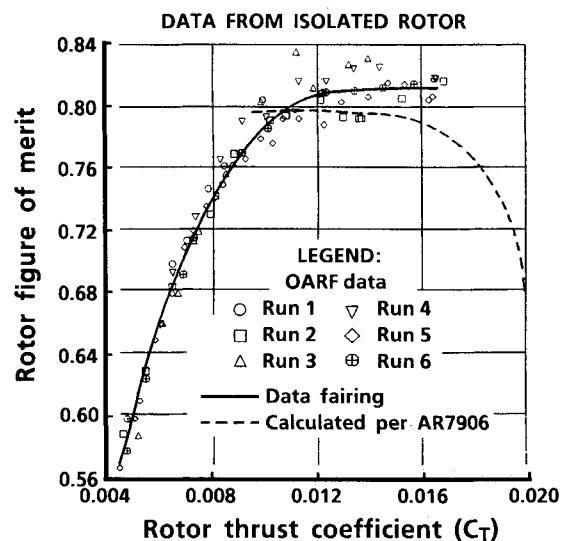


Fig. 1 The momentum element method underpredicts the figure of merit at high thrust levels.

Presented at AIAA Paper 89-1814 at the AIAA 20th Fluid Dynamics, Plasma Dynamics, and Lasers Conference, Buffalo, NY, June 12-14, 1989; received April 28, 1990; revision received Oct. 15, 1990; accepted for publication Dec. 1, 1990. Copyright © 1991 by Bell Helicopter Textron, Inc. Published by the American Institute of Aeronautics and Astronautics, Inc., with permission.

*Principal Engineer, Aerodynamic Computational Methods, Engineering Department, P.O. Box 482. Member AIAA.

†CFD Analyst, Industry Science and Technology Department, 1333 Northland Drive. Member AIAA.

and flowfield characteristics of rotorcraft blades at high thrust levels.

Advances have been made in the field of computational fluid dynamics (CFD) that now allow for the computation of the nonlinear flow characteristics about rotor blades. Only very recently have combined progress in algorithm development and computer memory size and speed allowed for a problem of the magnitude of a hovering rotor to be evaluated using CFD methods. Several computational fluid dynamic methods have been developed that can solve for the flow about helicopter rotor blades with differing levels of sophistication and complexity. Initially, potential flow methods were developed that allowed for the determination of pressure distributions, including compressibility effects on helicopter blades in the advancing region. First, quasi-steady methods were developed,³ followed by unsteady methods.⁴ Potential methods are constantly being upgraded to take advantage of improvements in solution methodology.^{5,6} These methods serve as the foundation of CFD analysis and design since they are fairly quick to run, do not require extremely large computer memory capabilities, and provide useful results for the helicopter advancing blade problem where viscous effects are small compared with compressibility effects.

Recently, methods have been developed that solve the Navier-Stokes equations for flow about rotor blades. These methods allow a numerical analysis of the complex, nonlinear flowfields around rotorcraft blades. Detailed analysis of the tip vortex formation in hover has been carried out by Srinivasan and McCroskey⁷ at NASA Ames using a Navier-Stokes solver. Another Navier-Stokes method, developed by Wake et al.⁸ (GIT3DNS), has been evaluated at high-speed forward-flight conditions.⁹ Although some preliminary work is being done to allow for the simultaneous evaluation of multiple blades,¹⁰ most CFD analysis codes for helicopters currently perform calculations on a single blade. Therefore, the influence of the wake of previous blades and wake distortions due to other bodies must be input into the current CFD blade analysis calculations.

Because these Navier-Stokes CFD methods compute details of the flowfield, they may be able to give insight into the aerodynamic phenomena that cause the discrepancies between the computed and measured thrust values of a highly loaded rotor. Understanding the mechanism that causes the increased thrusting capabilities over what is currently predicted would provide valuable insight and might allow the modification of new designs to take proper advantage of this flow phenomena. As grid details become more sophisticated and turbulence models become more reliable, accurate calculations of the performance of highly twisted rotor blades near stall will be possible.

Based on the desire to gain physical insight into high thrust rotor blade characteristics, an experiment is being performed to determine the ability of one current state-of-the-art CFD code to predict and explain hovering blade stall flow characteristics. The research work described here represents the first published attempt to use a three-dimensional Navier-Stokes solver to compute high thrust characteristics on a rotorcraft blade in hover. An immense amount of data was generated during this initial phase of the study, which has not all been evaluated in detail. This paper represents a status report of the findings from the evaluations that have been performed to date.

Objective

Accurate analytical predictions of hover performance have been a challenge to the rotorcraft aerodynamicist, especially for highly twisted rotors at high thrust levels where rotating flow phenomena increase the thrust over what would be predicted using lifting surface methods.¹¹ The objective of this paper is to show that a Navier-Stokes method gives insight into the marked increase in lift coefficients obtained near the stall of rotating blades, especially near the inboard section of

the blade. Several wind tunnel tests have measured this inboard lift increase.¹²⁻¹⁴ It is currently assumed that this phenomenon is due to separation being delayed to larger angles of incidence because of Coriolis forces in the rotating system.¹⁵ Results computed by a three-dimensional unsteady Navier-Stokes method for the flowfield about an axial flow rotor at high thrust levels will be presented. This condition was chosen since experimental results indicate that the delayed separation phenomenon was created in this case. In addition, axial flow hovering flight is a critical operating condition for VTOL aircraft, since hover performance usually determines the maximum payload of the rotorcraft vehicle.

Navier-Stokes Code

The governing equations as well as the computational method used in this study have been published in the open literature.^{8,16,17} The method is a strong conservation formulation of the full Reynolds-averaged Navier-Stokes equations that solve the unsteady, compressible, three-dimensional equations in a body-fitted coordinate system for the flow about a helicopter rotor blade.

Turbulence effects are accounted for through the notion of an eddy viscosity and thermal conductivity that appear as a result of the Reynolds averaging. The algebraic turbulence model developed by Baldwin and Lomax¹⁸ is used to evaluate eddy viscosity.

Discretization of the governing equations results in a consistent approximation to the conservation laws. The Navier-Stokes system of equations are solved on a structured computational mesh. The system of equations is integrated in time using the implicit Beam-Warming¹⁹ alternating-direction implicit (ADI) algorithm. However, the ADI splitting is implicit only in the wraparound and normal (ξ , η) plane normal to the spanwise (ζ) direction. This enables the solver to march through the span stations explicitly, performing implicit computations at each station. To reduce possible biasing errors, the sweep direction in the spanwise direction is reversed after every complete sweep through the grid planes.

Second-order finite-difference expressions are used for spatial derivatives, whereas first-order differences are used for temporal terms. Second-order implicit and fourth-order explicit dissipation is used to provide numerical stability. The viscous terms are also modeled in an explicit manner by keeping these terms on the right-hand side of the equation. This explicit treatment of the viscous terms reduces the computational effort required.¹⁶

The computational grid used in the present application is constructed from two-dimensional C-type wraparound grids that are stacked radially to produce a C-H grid topology. The C-grid normal to the rotor is generated algebraically using the sheared parabolic technique of Jameson.²⁰ For rotor blade calculations, the innermost span station is placed outboard of the symmetry plane. For the cases evaluated in this study, the innermost span station was located at an r/R of 0.150. The grid is attached to the blade, thus it rotates and translates with the blade. For the case of hover, the problem reduces to a steady one since the flow is identical at every azimuth location. The velocity of any given grid point with respect to the inertial system for the hover case can be determined by

$$X_r = -\Omega_y$$

$$Y_r = \Omega_x$$

$$Z_r = 0.0$$

All the contributions to the effective angle of attack, including collective pitch, built-in twist, elastic twist, and total inflow from induced velocities, are included by twisting the grid system. The grid at each defining station was deflected to the effective angle of attack based on computations from a lifting surface program that computes wake effects on the lift distribution.²¹

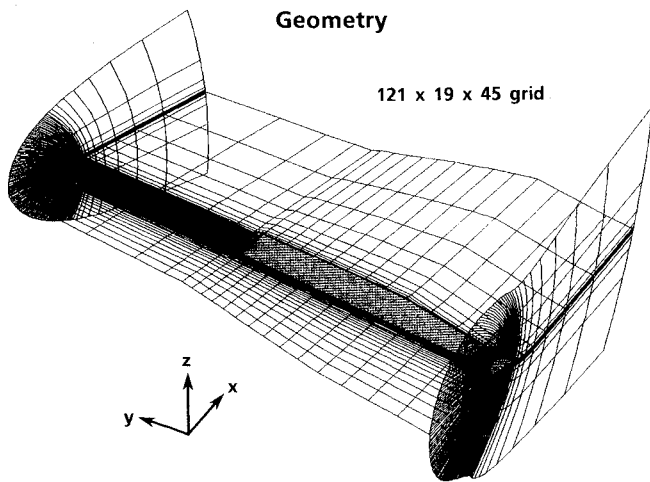


Fig. 2 A C-H grid topology defines the computational fields.

For the cases evaluated in this study, a total of 121 wrap-around grid points by 19 spanwise grid points by 45 normal grid points were used to define the computational field. Fourteen of the 19 spanwise grid points were located on the blade, and 10 points defined the wake slit. The 45 grid points in the normal direction were set such that the first point off the solid surface, within the boundary layer, was at 0.11% of chord. A graphical representation of the grid system used in this analysis is given in Fig. 2. In this figure, a representation of the first and last C-grid is shown along with a cut in the plane of the rotor showing the spanwise distribution of the stacked C-grids.

Experimental Data

An experimental investigation was conducted at the NASA Ames Research Center OARF to accurately measure the hover performance of a 0.658-scale model of the V-22 Osprey rotor.²² The test configurations included rotor only, rotor and image plane, and rotor, wing, flap, and image plane configurations. However, for this evaluation, the rotor-only measured data from Run 6 is compared to the Navier-Stokes code results. Run 6 was chosen since the air wind speed was very low during this run, and the measured data compared well to the fairing through all of the data that was measured during the rotor testing given in Fig. 1.

The tested rotor has three blades with a diameter of 7.62 m and was mounted horizontally on the test rig as depicted in Fig. 3. The balance system used at this facility was designed to be very sensitive to rotor thrust and torque, with minimal interactions caused by other forces, moments, or thermal effects.

For this paper, the computational results are compared to the OARF results for Run 6 of the V-22 0.658-scale model test. This case has a constant tip Mach number of 0.68 and low wind conditions. The collective angle was varied from 5 to 16.5 deg during this run.

Test/Theory Evaluations

All the computations for this study were performed on a CRAY X-MP/48 computer located at CRAY Research in Mendota Heights, Minnesota. Converged results were obtained in about 1200 cycles for most cases, requiring about 1.5 h of computer time for each solution. This number of cycles was sufficient to reduce the residuals by four orders of magnitude and to reduce oscillations in the lift and drag coefficient values to negligible levels.

Several different Navier-Stokes code cases were run for this study, and four cases were run at the specific conditions representing experimental test points with the collective angle being the independent variable. However, as the collective angle is changed, the distribution of inflow angle is also changed

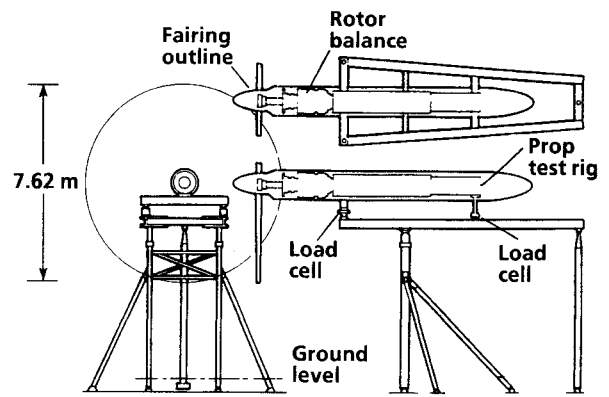


Fig. 3 The NASA Ames outdoor aerodynamic research facility test rig is mounted horizontally.

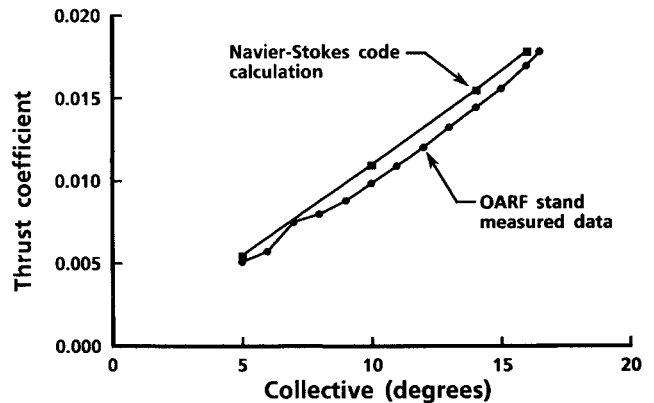


Fig. 4 The Navier-Stokes code predicts the thrust that was measured in the experiment.

so that the effective angle of attack values must also be varied. To provide the input effective angles of attack, a prescribed wake lifting surface method²¹ was run corresponding to the OARF V-22 0.658-scale test conditions. The effective angle of attack results from this code were used as input to the three-dimensional Navier-Stokes cases.

Figure 4, which is a comparison of the Navier-Stokes code results to the experimental data for thrust coefficient as a function of blade collective pitch angle, shows that the Navier-Stokes code can calculate thrust as a function of blade collective pitch angle that compares well to measured results. The difference in measured and computed thrust values is approximately 6% of measured thrust. It should be noted that the inflow angle as a function of radial station must be input to produce these results. In fact, some of the difference between the Navier-Stokes results and the measured data is likely to be due to the inaccuracy of the wake model used to set the effective angle of attack distribution.

The thrust distribution on the blade from the Navier-Stokes solution is given for four different blade collective pitch angles in Fig. 5, which indicates that the peak of the thrust distribution moves outboard as the collective is increased for this highly twisted rotor blade. This type of result is also produced by the lifting surface program that generated the effective angles of attack as shown in Fig. 6. For Figs. 5 and 6, equivalent collective angle results are shown. Figure 7 shows a comparison of the drag per foot as a function of blade radial station at a collective angle of 14 deg. The Navier-Stokes solution is significantly higher than the result from the lifting surface code. Researchers in CFD applications for aerospace technology realize that the drag values obtained from Navier-Stokes solvers are usually higher than equivalent experimental data. This delta has generally been ascribed to the grid density, turbulence modeling, and the transition criterion used by the solver. Studies have shown that the correct lift can be

0.658 scale V-22 blade Navier-Stokes analysis

Azimuth = 0.0000 deg
Tip speed = 755.00 ft/sec

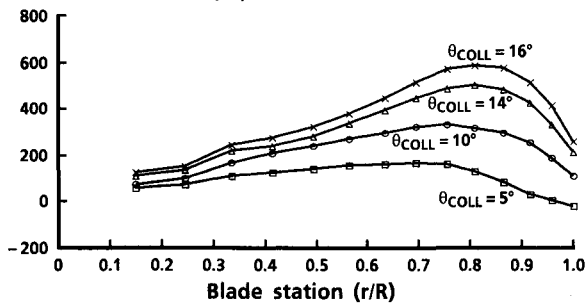


Fig. 5 Thrust distribution moves outboard as the collective is increased.

0.658 scale V-22 blade momentum element analysis

Azimuth = 0.0000 deg
Tip speed = 755.00 ft/sec

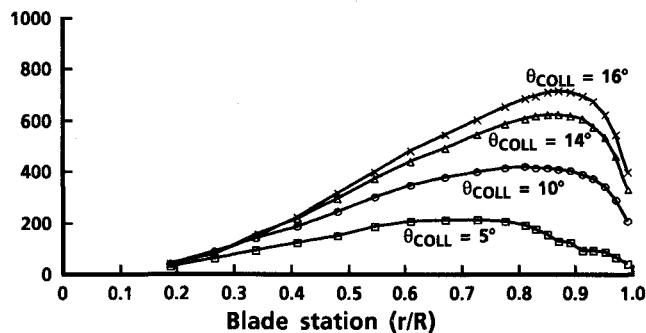


Fig. 6 The trend in thrust distribution as a function of collective angle from the lifting surface code is similar to the N-S results.

Azimuth = 0.0000 deg
Tip speed = 755.00 ft/sec

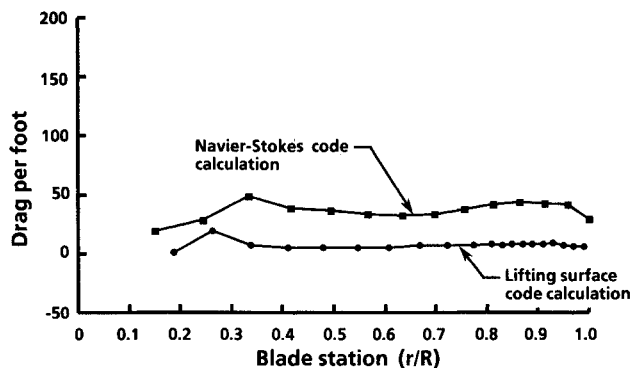


Fig. 7 The N-S code predicts higher drag per foot than the lifting surface code for the grid density used in this study.

computed with many fewer grid points than are required to achieve accurate drag values.²³ With a density of 121 wrap-around and 45 normal points, the Navier-Stokes solution for the case studied here is unable to resolve the drag accurately. The Baldwin-Lomax algebraic turbulence model, which is used in this Navier-Stokes solver, is also noted for its tendency to overpredict drag. The profile drag data for the lifting surface code solution is based on measured two-dimensional airfoil test data that have some small regions of laminar flow near the leading edge. This Navier-Stokes solver uses turbulent computations for the entire surface of the blade. All these factors contribute to high drag computations for the case investigated in this study.

The lift coefficient distribution from the Navier-Stokes solution is compared to a distribution computed using a lifting surface method for a total thrust coefficient of about 0.0155 in Fig. 8. It indicates that the Navier-Stokes method predicts

Azimuth = 0.0000 deg
Tip speed = 755.00 ft/sec

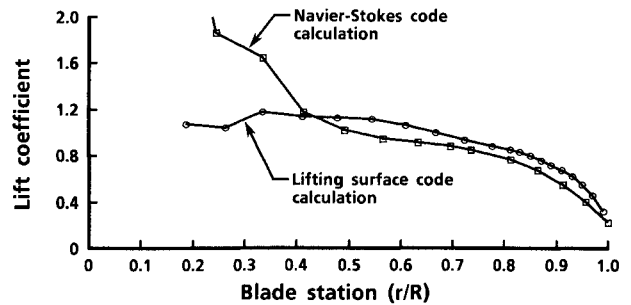


Fig. 8 The N-S code predicts a higher lift in the inboard region compared to a lifting surface code.

a much higher lift coefficient in the inboard region compared to the lifting surface method results at an equivalent thrust level. This difference in the inboard lift coefficient has been observed experimentally by other investigators¹¹⁻¹³; it has been attributed to spanwise flow velocities that effectively thin the boundary-layer separation region on the blade surface in the inboard region.¹¹ However, the Navier-Stokes results that were produced during this study indicate that the three-dimensionality of the flow allows the flow to remain attached to very high angles of attack. No outward radial flow velocities were observed in the inboard region of the blade over the collective range that corresponds to the test results.

That solution emulates the results of Banks and Gadd,²⁴ who showed why the boundary layer can stay attached near the center of rotation of a blade experiencing laminar flow. They were able to obtain a set of boundary-layer equations from the Navier-Stokes equations that captured the relationship between the chordwise and radial flows on a rotating blade. The Coriolis force terms in the chordwise equation and the centrifugal force terms in the radial equation were coupled by the rotation speed of the blade. Using integral boundary-layer methods, they were able to compute the laminar separation point on a rotating blade with linear adverse external velocity gradient. The separation points were computed for several rates of adverse gradient and indicated that rotation has the effect of postponing the laminar separation point. The amount of delay varies with the radius and is strongest for the inboard stations. In fact, their theory predicts that at certain inboard stations, the boundary layer will be stabilized completely against separation in a linearly decelerating flow on a rotating blade. The results from calculations performed during the Navier-Stokes code evaluations in the present study indicate that this phenomenon also occurs for turbulent flows.

Figure 9 shows velocity vectors near the surface of the blade at a radial location of $r/R = 0.24$ for a collective angle of 16 deg. At this condition, blade element theories indicate that this section would be separated; but as can be seen in the figure, the Navier-Stokes code predicts that no separation is produced on the inboard end of the blade. At a radial location of 0.75, there is also no separation predicted for this condition, as is shown in Fig. 10. Momentum element methods also predict that there is no separation at this station for the 16-deg collective angle. At a collective angle of 16 deg, the Navier-Stokes code trends agree with the momentum element code trends on the outboard end of the blade and disagree on the inboard end of the blade.

Higher collective angles were run using both the Navier-Stokes code and the momentum element code. At a collective angle of 24 deg, the momentum element solution indicates that the blade is completely separated from the inboard to outboard end. The Navier-Stokes code was run at this collective angle to see what solution would be produced. The velocity vectors near the surface of the blade at a radial location of $r/R = 0.24$ and a collective angle of 24 deg is shown

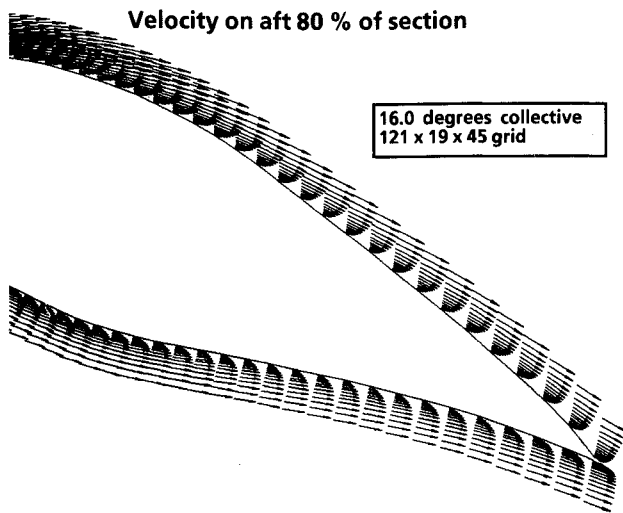


Fig. 9 The N-S code does not compute flow separation at $r/R = 0.24$ for collective angle of 16 deg even though the blade element method does predict separation.

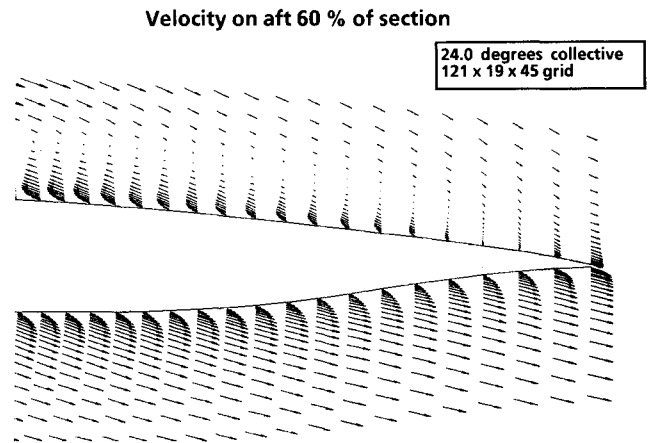


Fig. 12 For $r/R = 0.75$, the N-S code predicts separated flow at a collective angle of 24 deg.

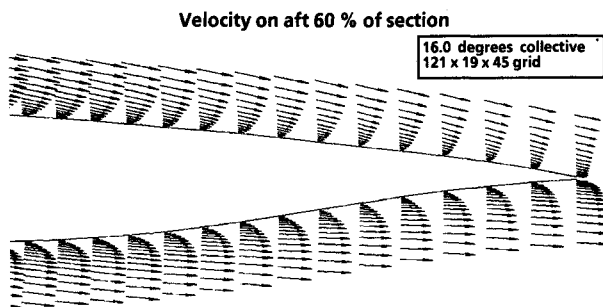


Fig. 10 The N-S code and the blade element code agree that there is no separation at $r/R = 0.75$ for collective angle of 16 deg.

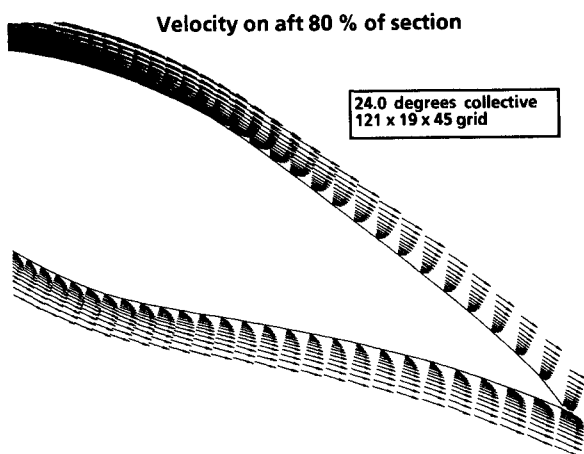


Fig. 11 Even at the extreme collective angle of 24 deg, no separation is predicted by the N-S code at $r/R = 0.24$.

in Fig. 11. It indicates that even at this extreme collective angle, the inboard end of the blade is not separated. At a radial location of $r/R = 0.75$, there is massive separation predicted for this condition, as shown in Fig. 12. Thus, the Navier-Stokes code predicts that flow separation is eliminated on the inboard end of this highly twisted blade. The elimination of the flow separation causes the achievable lift to be higher than that predicted by the momentum element methods that predict separation on the inboard end of the blade at collective angles of 10 deg and above.

The Navier-Stokes results that were produced during this study indicate that the three-dimensionality of the flow allows the flow on the inboard end of the blade to remain attached to very high angles of attack. This result is consistent with

results of Dwyer and McCroskey²⁵ and Banks and Gadd.²⁴ Both of these studies indicated that near the hub of a rotating blade no separation will occur.

Concluding Remarks

A Navier-Stokes code is being used to investigate the flow phenomena that cause the increase in lift coefficients obtained near the stall of a rotating blade. Results indicate that flow separation in the inboard region is curtailed for a rotating blade. This yields higher lift than that computed using blade element methods with two-dimensional airfoil data providing lift at the computed effective angle of attack. Although this result is useful in the explanation of the higher-than-predicted performance of the V-22 rotor blade in hover, there are several additional tasks that need to be performed to research this problem fully. First, as has been discussed, no systematic study of the grid density or inboard grid boundary was carried out in this case. Also, the effect of a centerbody was not included. At the intersection of the blade with the centerbody, very complex viscous flow phenomena such as flow separation and formation of a horseshoe vortex can occur. These factors may affect the inboard loading somewhat, but wind tunnel tests such as those of Himmelskamp¹² and Bass¹³ show that they will not eliminate the high lift coefficients produced on the inboard region of the blade.

Because of their ability to model details of the flow, it is anticipated that advanced CFD methods will make significant contributions to the understanding of the flow about rotorcraft vehicles in the near future.

Acknowledgments

The support of CRAY Research, Inc., is gratefully acknowledged for providing the computer resources used for this study. The authors would also like to thank L. N. Sankar of the School of Aerospace Engineering, Georgia Institute of Technology, for providing the original three-dimensional Navier-Stokes procedure that forms the basis of the BELLTECH code. Finally, the authors wish to thank Don Axley, Javier Camba, John Corrigan, Chuck Gatlin, Rick Reinesch, Matt Scott, and Kevin Spaight of Bell Helicopter Textron, Inc., for their technical assistance during the preparation of this paper.

References

- Harris, F. D., "Preliminary Study of Radial Flow Effects on Rotor Blades," *Journal of the American Helicopter Society*, Vol. 11, No. 3, 1966, pp. 1-21.
- Felker, F. F., Maisel, M. D., and Betzina, M. D., "Full Scale TiltRotor Hover Performance," *41st Annual Forum Proceedings*, American Helicopter Society, Alexandria, VA, May 1985, pp. 501-513.

³Arieli, R., and Tauber, M. E., "Computation of Subsonic and Transonic Flow About Lifting Rotor Blades," AIAA Paper 79-1667, Aug. 1979.

⁴Chang, I. C., "Transonic Flow Analysis for Rotors, Part II: Three Dimensional, Unsteady, Full Potential Calculation," NASA TP-2375, Jan. 1985.

⁵Strawn, R. C., and Caradonna, F. X., "A Conservative Full Potential Model for Unsteady Transonic Rotor Flows," *AIAA Journal*, Vol. 25, No. 2, Feb. 1987, pp. 193-198.

⁶Prichard, D. S., and Sankar, L. N., "Improvements in Transonic Flowfield Calculations," *44th Annual Forum Proceedings*, American Helicopter Society, Alexandria, VA, June 1988, pp. 785-796.

⁷Srinivasan, G. R., and McCroskey, W. J., "Navier-Stokes Calculations of Hovering Rotor Flowfields," AIAA Paper 87-2629-CP, August 1987.

⁸Wake, B. E., Sankar, L. N., Wu, J., and Ruo, S. Y., "An Efficient Procedure for the Numerical Solution of Three-Dimensional Viscous Flows," AIAA Paper 87-1159, June 1987.

⁹Narramore, J. C., Sankar, L. N., and Vermeland, R., "An Evaluation of a Navier-Stokes Code for Calculations of Retreating Blade Stall on a Helicopter Rotor," *44th Annual Forum Proceedings*, American Helicopter Society, Alexandria, VA, June 1988, pp. 797-808.

¹⁰Chen, C. L., McCroskey, W. J., and Ying, S. X., "Euler Solution of Multiblade Rotor Flow," Paper No. 2-2, 13th European Rotorcraft Forum, Arles, France, Sept. 1987.

¹¹Milborrow, D. J., "Changes in Aerofoil Characteristics Due to Radial Flow on Rotating Blades," 7th Annual Workshop, British Wind Energy Association, Oxford, England, March 1985.

¹²Himmelskamp, H., "Profile Investigations on a Rotating Airscrew," *Reports and Translations*, No. 832, M. A. P. Völknerode (MAP-VG 177-T), Sept. 1947, translated from "Profiluntersuchungen an einem umlaufenden Propeller," Dissertation, Göttingen 1945; Mitt. Max-Planck-Institut für Strömungsforschung Göttingen Nr. 2 (1950).

¹³Bass, R. M., "Small Scale Wind Tunnel Testing of Model Propellers," AIAA Paper 86-0392, Jan. 1986.

¹⁴Tung, C., and Branum, L., "Model Tilt-Rotor Hover Performance and Surface Pressure Measurement," *46th Annual Forum Proceedings*, Vol. II, American Helicopter Society, Alexandria, VA,

May 1990, pp. 785-796.

¹⁵Schlichting, H., "Boundary Layers on Rotating Bodies," *Boundary-Layer Theory*, 7th ed., McGraw-Hill, New York, 1979, pp. 649-651.

¹⁶Wake, B. E., and Sankar, L. N., "Solutions of the Navier-Stokes Equations for the Flow about a Rotor Blade," *Proceedings of the National Specialists' Meeting on Aerodynamics and Aeroacoustics*, American Helicopter Society, Alexandria, VA, Feb. 1987.

¹⁷Malone, J. B., and Narramore, J. C., "BELLTECH—A Multi-Purpose Navier-Stokes Code for Rotor Blade and Fixed-Wing Configurations," *45th Annual Forum Proceedings*, American Helicopter Society, Alexandria, VA, May 1989, pp. 297-310.

¹⁸Baldwin, B. S., and Lomax, H., "Thin-Layer Approximations and Algebraic Model for Separated Turbulent Flow," AIAA Paper 78-257, June 1978.

¹⁹Beam, R. M., and Warming, R. F., "An Implicit Factored Scheme for the Compressible Navier-Stokes Equations," *AIAA Journal*, Vol. 16, No. 4, April 1978, p. 393-402.

²⁰Jameson, A., "Iterative Solution of Transonic Flows over Airfoils and Wings Including Flows at Mach 1," *Communications in Pure and Applied Mathematics*, Vol. 27, 1974, p. 283-309.

²¹Kocurek, J. D., Berkowitz, L. F., and Harris, F. D., "Hover Performance at Bell Helicopter Textron," *36th Annual Forum Proceedings*, American Helicopter Society, Alexandria, VA, May 1980, Preprint No. 80-3.

²²Felker, F. F., Signor, D. B., Young, L. A., and Betzina, M. D., "Performance and Loads Data From a Hover Test of a 0.658-Scale V-22 Rotor and Wing," NASA TM 89419, April 1987.

²³Rumsey, C. L., "Parametric Study of Grid Size, Time Step, and Turbulence Modeling on Navier-Stokes Computations Over Airfoils," AGARD 62nd Meeting of the Fluid Dynamics Panel Symposium on Validation of Computational Fluid Dynamics, Paper No. 5, AGARD-AR-257, Lisbon, Portugal, May 2-5, 1988.

²⁴Banks, W. H. H., and Gadd, G. E., "Delaying Effect of Rotation on Laminar Separation," *AIAA Journal*, Vol. 1, No. 4, April 1963, p. 941-942.

²⁵Dwyer, H. A., and McCroskey, W. J., "Crossflow and Unsteady Boundary Layer Effects on Rotating Blades," AIAA Paper 70-50, January 1970.